2019 16th International Conference on Electrical Engineering, Computing Science and Automatic Control (CCE).
Mexico City, Mexico. September 11-13, 2019

Fixed-time robust output feedback control of a restricted state biped robot based on a tangent barrier Lyapunov function

Karla Rincon
Automatic Control Department
CINVESTAV-IPN
krincon@ctrl.cinvestav.mx

Isaac Chairez
Bioprocesses Department
UPIBI-IPN
jchairezo@ipn.mx

Wen Yu
Automatic Control Department
CINVESTAV-IPN
yuw@ctrl.cinvestav.mx

***Abstract*—The aim of this study is developing a robust controller with state dependent gains which guarantees the fixed-time robust convergence of the tracking error trajectories at each articulation for a suspended biped robot. The satisfaction of the state restrictions is justified with the controller gains design that are calculated using a Barrier tangent-type Lyapunov candidate function. The explicit adaptation law is obtained with the analysis of the controlled variant of the Barrier function, including the deviation terms for the selected adaptive gains. The virtualized model of the biped robot serves as a testing platform for the suggested controller, this computer-aided model robot operates as numerical test bench for the robust constraint controller. Some numerical simulation demonstrate the application of the state feedback controller with state restrictions and the gain law. The comparison of the tracking performance implementing the suggested controller and the regular proportional-integral-derivative form confirms the origin as a fixed-time stable equilibrium point for the tracking error while the state space restrictions are satisfied.**

I. Introduction

Automatic controllers aimed to regulate biped robots have been developed for many years. Taking the human gait cycle as reference, many control strategies could enssure the secure headway of the biped structure. Most of these controllers have used the Zero Moment Point (ZMP) [1] as main stability criterion, which considers the sum of gravitational and inertia forces with the goal of forcing the moment of inertia equal to zero. While the reference point corresponding to the center of mass of the biped robot remains inside a support polygon, the robot balance is ensured. This restriction can be only satisfied with the application of robust controllers which may satisfy the tracking of reference trajectories that corresponds to the adequate sequence of articulation movements. Such restrictions may be used to design the so-called stable gait cycle for an autonomous biped robot. Notice that most of the ZMP-based strategies consider asymptotic controllers for ensuring the satisfaction of the polygon restriction. Also, many of them did not take into account the articulation angular restrictions which are natural in biped robots designs. In addition, the strategies mentioned previously require a proper gain tuning that usually is a high time consuming process, which can provoke the robot may realize undesired movements along the transient period of the controller exertion.

Finite and fixed time convergences are desirable for state constraint systems (such as the biped robot) with the suitable automatic control designs [2]. This requirement arises from the natural strict time restrictions that may appear in several real plants, where the operating time could be of finite-duration [3]. Nowadays, finite as well as fixed time convergences appear as a consequence of introducing set-valued functions like sign function, as part of the controller. Most of the control designs that use sign functions are included in the well-developed sliding-mode theory [4], [5], [6]. In general, sliding-mode controls stirred the states of the system under analysis to a given manifold even in augmented state spaces such as in the case of high-order sliding modes. Even more, the introduction of nonlinear sliding surfaces contributes to regulate the converge velocity of the states once they are on the sliding manifold [7], [8]. The majority of systems that can be controlled by sliding-mode controllers and still ensuring the finite or fixed time convergences are state or output based linearizable systems with finite relative degree for the available output [9], [10]. For such class of systems, the theory describing how to design the controllers is really mature. However, there is a limited number of studies describing how to implement sliding-mode controllers where the states are restricted with known bounds in advance [11].

The application of the Barrier Lyapunov function (BLF) can be an option to take into account the presence of articulation restricted movement. The number of BLF applications is growing over the last years. Different types of BLF appeared recently including the logarithmic, integral and tangent to mention just a few of them. However, there is still a necessity of showing the finite-time convergence of the state trajectories when the BLF is considered as stability analysis tool. One option is the application of polynomial controllers which may force a non-Lipschitz dynamics near the origin. This class of controllers may not show robustness against non-vanishing perturbations but still can offer a reliable operation near the equilibrium point.

The main contribution of this study is the development of a robust controller estimated with the stability analysis based on a controlled BLF. A novel class of tangent BLF justifies the fixed-time convergence of the tracking error between the articulation angles and the corresponding reference trajectories. The stability proof provides the gains adjustment conditions for the controller. Some numerical evaluations, considering the application of a virtualized biped robot as testing system, confirmed that the controller may offer the stability conditions emerging from the application of the BLF.

This manuscript is organized as follows. Section II presents the description of the robot structure including its suggested mechanical structure. Section III describes the proposed adaptive controller based on the tangent-like BLFs together with the corresponding proof. The numerical evaluations of

978-1-7281-4840-3/19/$31.00

the controller are presented in Section IV, where the proposed controller is compared against a classical PID controller. Finally, in the section V, the conclusion of this paper is presented.

II. The biped robot

This section presents the components forming the proposed robot structure. First of all, the general arrangement of linear actuators yielding the joints configurations is described.

The biped robot was designed to satisfy the regular values for gait descriptors [12]: step length $72cm/s$, cadence $1.87steps/s$ and walking speed $1.37m/s$ for a person 180 cm tall.
The structure can be divided in two sections: 1) the hip that connects both legs and is 33.81 cm length, 2) and the bilaterally symmetric legs, divided by the knee joint in 45.72 cm thigh, and 41.19 cm leg as shown in the Figure 1 *a)*.

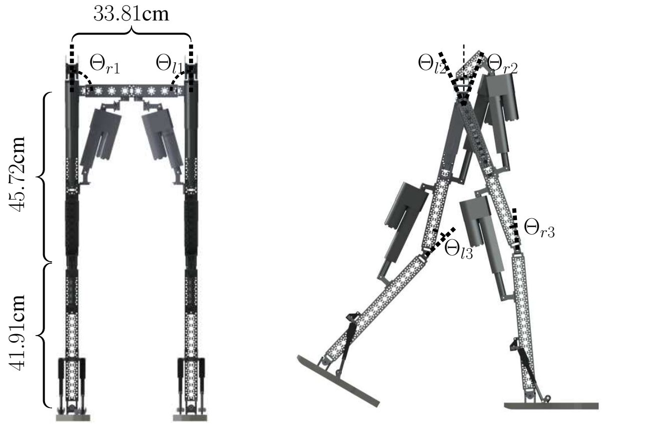

a) Frontal view a) Sagittal view

Fig. 1. Dimensions and degrees of freedom considered in the structure of the biped robot

In view of the angular displacements that the robot must track to exert a natural walk, the proposed biped robot considers six degrees of freedom (DOF) in two anatomical planes. Its simplified layout has two joints at the hip to reach the abduction/adduction and flexion/extension movements. Table I [12], contains a brief report of the expected articulation displacements for each joint. These displacements correspond to the robot configuration presented in Figure 1.

TABLE I
Range of movement considered for the robot

	Saggital plane	
	Maximum	Minimum
Hip	35°	-10°
Knee	60°	5°

The simulated joint structure is based on actual bearings attached to aluminum links. The arrangement of the joint transforms the linear movement from the actuators to angular movements. This configuration appears as an additional contribution of this study, which is considering a simplified instrumentation option. This design strategy has the aim of providing a robust mechanical structure for the robot arrangement.

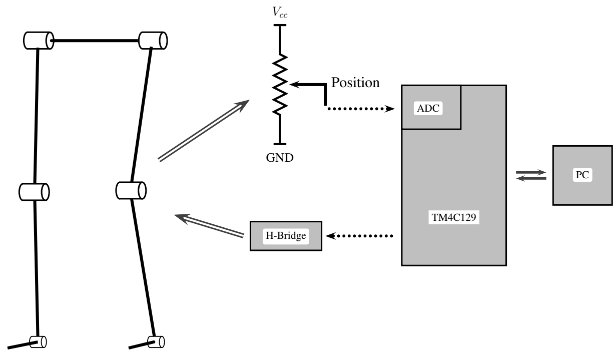

Fig. 2. Electronic instrumentation arrangement

The hypotetic instrumentation (Figure 2) considers the measurement of the joint displacement. The supposed technical elements used to mobilize the joints are linear actuators. The mechanical characteristics considered in the election of the actuators are: the displacement at maximum load is $3.5cm/s$, the dynamic thrust is $11.34KgF$, the static load $226.8KgF$ and spindle type is 3mm pitch, single thread. Complementary, the electrical characteristics of the engines are: voltage range is 6 to $12V$, and the current consumption at maximal load is $3.8A$. Embedded in the linear actuators are $10K\Omega$ variable resistors used as position sensors, they have $\pm5\%$ of tolerance. The angular movement is linearly dependent of the shank displacement. The motor drivers are the ST's™IC VNH5019 AC-DC two branches power converter in the Pololu's™carrier board. It operates form 5.5 to $24V$, deliver $12A$ continuously and works with $2.5-5V$ logic levels, also, supports $> 20KHz$ PWM signals. It has build-in protection against reverse-voltage, over-voltage, under-voltage, over-temperature, and over-current.

This suggested instrumentation provides the inspiration to design the proposed controller assuming the natural restrictions coming from the real operation conditions of the biped device. Also, the proposed embedded digital instrumentation defines the processing capacities to implement the controller. All these elements were considered within the numerical analysis of the controller application.

In order to process the digital signals, it is chosen the Texas Instruments'® TIVA Evaluation Board with TM4C129 MCU possess a 120MHz 32-bit ARM Cortex-M4 CPU, dual 12-bit 2MSPS ADCs and 1MB Flash, 256KB SRAM, 6KB EEPROM. All of these characteristics enables the in-chip numerical implementation of the proposed controller, preventing the design of a non-realizable controller which cannot be applied in real robot.

III. Output feedback control

A biped robot system can be mathematically represented in a compact form as [13], [14]:

$$\begin{aligned} \frac{d}{dt}x_\alpha(t) &= x_\beta(t) \\ \frac{d}{dt}x_\beta(t) &= f\left(x(t),t\right) + g\left(x_\alpha(t)\right)u(t) + \zeta\left(x(t),t\right) \end{aligned} \tag{1}$$

with $x^\top = [x_\alpha^\top, x_\beta^\top]$, where $x \in X \subset \mathbb{R}^{2n}$, X an open subspace, $x_\alpha \in \mathbb{R}^n$ is the vector of angles that describes the angular movements at each joint of the biped robot. The vector $x_\beta \in \mathbb{R}^n$ represents the time derivative of the angular displacements for each joint.

The function $f : X \times \mathbb{R}^+ \rightarrow \mathbb{R}^n$ is a vector field that represents the internal dynamics of the biped robot, its structure can be obtained by using Euler-Lagrange method. In this manuscript it is not thoroughly studied the interactions between the contact surface and the biped structure. The properties of the f function guarantee validity of the locally Lipschitz condition:

$$\begin{gathered}\|f\left(x^1\right) - f\left(x^2\right)\| \leq L_f\|x^1 - x^2\|,\\ x^1 \in X, x^2 \in X, L_f \in \mathbb{R}^+\end{gathered} \tag{2}$$

The function $g : \mathbb{R}^n \rightarrow \mathbb{R}^{n\times n}$ describes how the input vector affects the dynamics of the biped robot. This structure owns a well defined inverse since the inertia matrix of the biped robot is positive definite and satisfies the inequality (3) uniformly on $t \geq 0$, where it is used the Frobenious matrix norm:

$$\begin{gathered}0 < g^- \leq \|g\left(x_\alpha\right)\|_F \leq g^+ < +\infty\\ g^- \in \mathbb{R}^+, g^+ \in \mathbb{R}^+\end{gathered} \tag{3}$$

The term $\zeta : X \times \mathbb{R}^+ \rightarrow \mathbb{R}^n$ represents the uncertainties/perturbations, and it belongs to the following set:

$$\Xi = \left\{\zeta | \sup_{t\geq 0,\ x\in\mathbb{R}^n} \|\zeta\|^2 \leq \zeta_0 + \zeta_1\|x\|^2\right\} \tag{4}$$

Because of the nature of the mechanical structure, it must satisfy the angular displacement restrictions for all the components of the state vector:

$$-\infty < x_{\alpha,i}^- \leq x_{\alpha,i} \leq x_{\alpha,i}^+ < +\infty,\ \ x_{\alpha,i}^-, x_{\alpha,i}^+ \in \mathbb{R} \tag{5}$$

It is assumed that exists an upper limit x^+, which is defined as:

$$\frac{(\max_i x_i^+)n}{\lambda_{min} P} = x^+ \tag{6}$$

where x_i defines the restriction for the i^{th} angular displacement and $P \in \mathbb{R}^{n\times n}$ is a positive definite weighting matrix. Such matrix can be used to restrict some specific articulations.

Then, x^+ defines the bounds for the states according to the following inequality:

$$\frac{\|x\|_P^2}{x^+} \leq 1 \tag{7}$$

A. Problem Statement

The main objective of this manuscript is to design a controller $u = u(t)$ for a biped robot such that

$$\|x_a(t) - x_a^*(t)\| \leq \varsigma \quad , \quad \forall t \geqslant \tau : 0 \tag{8}$$

where τ is a given time, ς is the quality of the tracking for the reference trajectory, x_a corresponds to the position of joints explained before and x_a^* to the target reference trajectories. The generalized coordinate x_a is defined as follows

$$x_a = |x_{a,i}|_{i=1:n}$$

B. Control design

To design the controller, let assume that a reference trajectory is proposed satisfying

$$\begin{gathered}\frac{d}{dt}x_\alpha^*(t) = x_\beta^*(t)\\ \frac{d}{dt}x_\beta^*(t) = h\left(x_\alpha^*(t), x_\beta^*(t), t\right)\end{gathered} \tag{9}$$

Where the function $h : X \times X \times \mathbb{R}^+ \rightarrow \mathbb{R}^n$ a locally Lipschitz function, which defines the reference state variables. Consider the tracking error $\Delta(t) \in \mathbb{R}^{2n}$ defined by $\Delta = x - x^*$, where $x^* = [(x_\alpha^*)^\top, (x_\beta^*)^\top]^\top$. Then, the dynamics of $\Delta(t)$ is given by:

$$\begin{gathered}\frac{d}{dt}\Delta(t) = A\Delta(t) + B\left(f\left(x(t), t\right) + g\left(x_\alpha(t)\right)u(t)\right)\\ +B\left(\zeta\left(x(t), t\right) - h\left(x_\alpha^*(t), x_\beta^*(t), t\right)\right)\end{gathered} \tag{10}$$

with the matrices A and B satisfying a companion controllable form of appropriate dimensions.

Let propose an adaptive controller that satisfies the following linear form

$$u(t) = g^{-1}(x_a(t))K(t)\Delta(t) \tag{11}$$

with the time-varying gain fulfilling the conditions:

$$\begin{gathered}\frac{d}{dt}K(t) = -2\lambda^{-1}\Bigg[c_1\tilde{K}(t)\left(\tilde{K}^\top(t)\tilde{K}(t)\right)^{-\frac{1}{p}} +\\ c_2\tilde{K}(t)\left(\tilde{K}^\top(t)\tilde{K}(t)\right)^{\frac{1}{p}} + \frac{p\pi}{2x^+}\cdot\Gamma(\Delta(t))B^\top P\Delta(t)\Delta(t)^\top\Bigg]\\ \Gamma(x(t)) = tan^{p-1}(z(\Delta(t))) + tan^{p+1}\left(z(\Delta(t))\right)\\ z(\Delta(t)) = \pi\frac{\|\Delta(t)\|_P^2}{4x^+} \qquad \tilde{K}(t) = K(t) - K^*\end{gathered} \tag{12}$$

with $\lambda \in \mathbb{R}^+$, the constants $c_1 = \left(\frac{\lambda\varrho p\pi}{x^+}\right)^{\frac{p-1}{p}}$, $c_2 = \left(\frac{\lambda\varrho p\pi}{x^+}\right)^{\frac{p+1}{p}}$, $\varrho \in \mathbb{R}^+$ and $p \in \mathbb{R}$, $p \in (0, 1]$, $K(0) = |k_s|_{s=1,\ldots,2n}, -\infty < k_s < 0$. The matrix $K^* \in \mathbb{R}^{m\times n}$ must be selected in such a way that $A + BK^*$ is Hurwitz with the matrix A may coming from the linear section of the biped robot mathematical model and the matrix B defines the input injection term in the robot dynamics. Using the extended Ackerman formula for multivariable systems [15], the matrix K^* can be estimated.

The following theorem provides the main result of this study corresponding to the gains conditions for the proposed controller which may guarantee the satisfaction of the state constrains for the biped robot operation while ensures the fixed time convergence of the tracking trajectories to the origin in a given finite time.

Theorem 1. *Given the class of nonlinear systems as in* (10) *with the control law* $u(t)$ *as in* (11) *with the time-varying gain* $K(t)$ *regulated by the adaptation law* (12)*. Let us assume that the uncertain section of the model* ζ *satisfies* (4)*. While* *it holds a positive scalar γ and constant matrix $K^* \in \mathbb{R}^{m\times n}$ such that the following matrix inequality*

$$\Sigma(P) < 0 \ \ subjected \ to \ (4)$$

$$\Sigma(P) = \begin{bmatrix} P(A_K+\gamma I_n)+(A_K+\gamma I_n)^\top P+\zeta_1 Q_x & PD \\ D^\top P & -Q_\zeta \end{bmatrix} \quad (13)$$

where $D = [0_{n\times n}, I_{n\times n}]$ has a positive definite and symmetric matrix P then the origin is a practically fixed-time stable equilibrium point for the tracking error $\Delta(t)$ with the attraction region given by $\|\Delta(t)\|_P^2 \geq \varsigma = 2\frac{\zeta_0}{\alpha}$ with $\alpha > 0$.

Proof. Let consider the Lyapunov Candidate Function as follows:

$$V(\Delta(t)) = tan^p\left(z(\Delta(t))\right) + \lambda tr\left\{\tilde{K}^\top(t)\tilde{K}(t)\right\} \quad (14)$$

The time derivative (Dini) of the Lyapunov Candidate Function satisfies

$$\frac{d}{dt}V(\Delta(t)) = p\cdot tan^{p-1}\left(z(\Delta(t))\right)\frac{d}{dt}tan\left(z(\Delta(t))\right) + 2\lambda tr\left\{\tilde{K}^\top(t)\frac{d}{dt}\tilde{K}(t)\right\} \quad (15)$$

where

$$\frac{d}{dt}tan\left(z(\Delta(t))\right) = \frac{\pi sec^2\left(z(\Delta(t))\right)}{2x^+}\Delta^\top(t)P\frac{d}{dt}\Delta(t) \quad (16)$$

In consequence, the following equation is valid for the derivative of the Lyapunov Candidate Function V:

$$\frac{d}{dt}V(\Delta(t)) = \frac{p\pi}{2\Delta^+(t)}\cdot\Gamma(x(t))\Delta^\top(t)P\frac{d}{dt}\Delta(t) + 2\lambda tr\left\{\tilde{K}^\top(t)\frac{d}{dt}K(t)\right\} \quad (17)$$

The term $\Delta^\top(t)P\frac{d}{dt}\Delta(t)$ requires the substitution of the $\Delta(t)$ dynamics given in (10), that is

$$\Delta^\top(t)P\frac{d}{dt}\Delta(t) = \Delta^\top(t)P\left(A\Delta(t) + B\left(w(t) + g\left(x_\alpha(t)\right)u(t)\right)\right)\Delta(t) \quad (18)$$

where $w(t) = f\left(x(t),t\right) + \zeta\left(x(t),t\right) - h\left(x_\alpha^*(t), x_\beta^*(t), t\right)$.

The equation (18) can be represented as follows:

$$x^\top P\frac{d}{dt}x = \frac{1}{2}\eta^\top(t)\begin{bmatrix} PA_K + A_K^\top P & PD \\ D^\top P & 0_{n\times n}\end{bmatrix}\eta(t) + \Delta^\top(t)PB\tilde{K}(t)\Delta(t) \quad (19)$$

where $\eta = \begin{bmatrix} x^\top & \zeta^\top\end{bmatrix}^\top$ and $A_K = A + BK^*$.

The inclusion of the upper-bound of the ζ introduced in (4) and taking into account that $\sigma_1^\top = \sigma_2 = tr\left\{\sigma_2\sigma_1^\top\right\}$ with $\sigma_1 \in \mathbb{R}^n$ and $\sigma_2 \in \mathbb{R}^n$ transforms the expression (19) into

$$\Delta^\top(t)P\frac{d}{dt}\Delta(t) \leq \frac{1}{2}\eta^\top\Sigma\eta + \zeta_0 + tr\left\{\tilde{K}(t)B^\top P\Delta(t)\Delta^\top(t)\right\} \quad (20)$$

Using the result obtained in (20) in the ordinary differential equation (17) gives

$$\frac{d}{dt}V(\Delta(t)) \leq \frac{p\pi}{2x^+}\cdot\Gamma(\Delta(t))\cdot \left[\frac{1}{2}\eta^\top\Sigma\eta + \zeta_0 - \alpha\Delta^\top(t)P\Delta(t)\right] + tr\left\{\tilde{K}(t)\left(\frac{p\pi}{2x^+}\cdot\Gamma(\Delta(t))B^\top P\Delta(t)\Delta^\top(t) + 2\lambda\frac{d}{dt}K(t)\right)\right\} \quad (21)$$

The reorganization of (21) introduces the adaptive law for the gain K as follows

$$\frac{d}{dt}V(x(t)) \leq \frac{p\pi}{2x^+}\cdot\Gamma(\Delta(t))\cdot \left[\frac{1}{2}\eta^\top\Sigma\eta + \zeta_0 - \alpha\Delta^\top(t)P\Delta(t)\right] + tr\left\{\tilde{K}^\top(t)\left(\frac{p\pi}{2x^+}\cdot\Gamma(\Delta(t))B^\top P\Delta(t)\Delta^\top(t) + 2\lambda\frac{d}{dt}K(t)\right)\right\} + tr\left\{c_1\left(\tilde{K}^\top(t)\tilde{K}(t)\right)^{\frac{p-1}{p}} + c_2\left(\tilde{K}^\top(t)\tilde{K}(t)\right)^{\frac{p+1}{p}}\right\} - c_1 tr\left\{\tilde{K}^\top(t)\tilde{K}(t)\right\}^{\frac{p-1}{p}} + c_2 tr\left\{\tilde{K}^\top(t)\tilde{K}(t)\right\}^{\frac{p+1}{p}} \quad (22)$$

Using the argument presented in (13) and considering the state condition $\|\Delta\|_P^2 \geq 2\frac{\zeta_0}{\alpha}$, one gets (with $\varrho > 0$)

$$\frac{d}{dt}V(\Delta(t)) \leq -\frac{\varrho p\pi}{2x^+}\cdot\Gamma(\Delta(t)) - c_1 tr\left\{\tilde{K}^\top(t)\tilde{K}(t)\right\}^{\frac{p-1}{p}} - c_2 tr\left\{\tilde{K}^\top(t)\tilde{K}(t)\right\}^{\frac{p+1}{p}} + tr\left\{c_1\tilde{K}^\top(t)\tilde{K}(t)\left(\tilde{K}^\top(t)\tilde{K}(t)\right)^{\frac{-1}{p}}\right\} + tr\left\{c_2\tilde{K}^\top(t)\tilde{K}(t)\left(\tilde{K}^\top(t)\tilde{K}(t)\right)^{\frac{1}{p}}\right\} + tr\left\{\tilde{K}^\top(t)\left(\frac{p\pi}{2x^+}\cdot\Gamma(x(t))B^\top P\Delta(t)\Delta^\top(t) + 2\lambda\frac{d}{dt}K(t)\right)\right\} \quad (23)$$

Using the definition of the energetic function proposed in (14) yields

$$\frac{d}{dt}V(\Delta(t)) = \frac{p\pi}{2x^+}\cdot\left(V^{\frac{p-1}{p}}(x(t)) + V^{\frac{p+1}{p}}(\Delta(t))\right)\cdot \Delta^\top(t)P\frac{d}{dt}\Delta(t) + 2\lambda tr\left\{\tilde{K}^\top(t)\frac{d}{dt}K(t)\right\} \quad (24)$$

Considering the triangle inequality for the p-norm, and using structure of the energetic function proposed (14) yields

$$\frac{d}{dt}V(\Delta(t)) \leq \frac{-\varrho p\pi}{2x^{+}} \cdot \left(V^{\frac{p-1}{p}}(\Delta(t)) + V^{\frac{p+1}{p}}(\Delta(t))\right) + tr\left\{c_1 \tilde{K}^{\top}(t)\tilde{K}(t)\left(\tilde{K}^{\top}(t)\tilde{K}(t)\right)^{\frac{-1}{p}}\right\} + tr\left\{c_2 \tilde{K}^{\top}(t)\tilde{K}(t)\left(\tilde{K}^{\top}(t)\tilde{K}(t)\right)^{\frac{1}{p}}\right\} + tr\left\{\tilde{K}^{\top}(t)\left(\frac{p\pi}{x^{+}} \cdot \Gamma(x(t))B^{\top}P\Delta(t)\Delta^{\top}(t) + 2\lambda\frac{d}{dt}K(t)\right)\right\} \tag{25}$$

If the adaptive law for the gain $\tilde{K}(t)$ given in (12) is considered in (25), then

$$\frac{d}{dt}V(\Delta(t)) \leq \frac{-\varrho p\pi}{2x^{+}} \cdot \left(V^{\frac{p-1}{p}}(\Delta(t)) + V^{\frac{p+1}{p}}(\Delta(t))\right) \tag{26}$$

Then evidently, $0 < \frac{p-1}{p} < 1$ and $\frac{p+1}{p} > 1$, then the origin is fixed-time practically stable according to the result presented in [16]. □

The fixed-time stability of the attraction region provided in Theorem 1 is a consequence of the growing behavior of $K(t)$ when $\Delta(t)$ approaches the boundary of the set.

Employing unbounded gain seems counter intuitive because we achieved fixed-time regulation with unbounded inputs. As illustrated by the controller structure, the product Kx in the control law is the scaled state which remains bounded, as the stability analysis based on the proposed energetic function confirms.

Remark 1. *If the set Ξ changes with $\zeta_0 = 0$, then the origin is fixed-time stable. This result is justified directly from the result attained in the Theorem 1 of this study.*

IV. Numerical Evaluations

A simplified representation of the robot, which is designed in the CAD software SolidWorks® with the parameters corresponding to the physical structure, is used as a testing model. The adaptive control law proposed in (11) was evaluated using MATLAB® in the environment Simulink®. The characteristics of the simulation are: fixed step at $10\mu s$ seconds, with solver Runge-Kutta. In order to compare the functioning of the proposed control, it was also implemented a classical PID controller in the structure. The comparison of the trajectory tracking is carry out in a single lower limb. The reference trajectories were designed to guarantee the ZMP criteria, which is also satisfied by the states of the biped robot with the application of the suggested controller.

Figure 3 demonstrates the tracking of the reference trajectory for the hip articulation of the biped robot. Notice that in comparison to the regular PID controller, the tracking of the reference is attained a couple of seconds latter. However, the PID is not able to provide (at least theoretically) the finite time and robust convergence of the tracking error to the invariant set described in the main result of this study.

Figure 4 provides the corresponding comparison for the knee trajectory. Notice that here the difference between the trajectories enforced by the evaluated controllers is less evident. Notice also that the given fixed-time convergence controller based on the Barrier Lyapunov function is not exhibiting high frequency oscillations as the regular siding mode controllers (or similar) do.

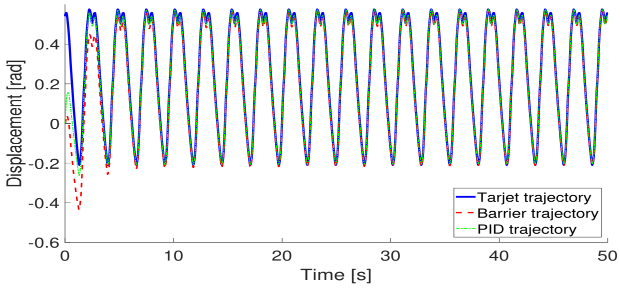

Fig. 3. Comparison of trajectory tracking performance between the proposed and PID controllers at the hip joint in the biped robot

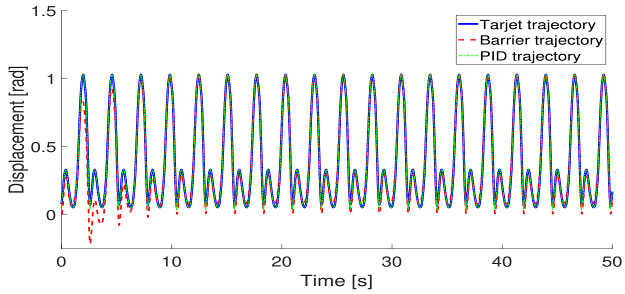

Fig. 4. Comparison of trajectory tracking performance between the proposed and PID controllers at the knee joint in the biped robot

Figures 5 and 6 depicts the logarithmic evolution of the control power needed to exert the tracking of the reference trajectories. This comparison shows a similar control consumption for both articulations. Moreover, notice that the Barrier controller tends to consume less energy if at the moments when the the reference trajectories change direction which is a remarkable characteristic in terms of the real operation of biped robots.

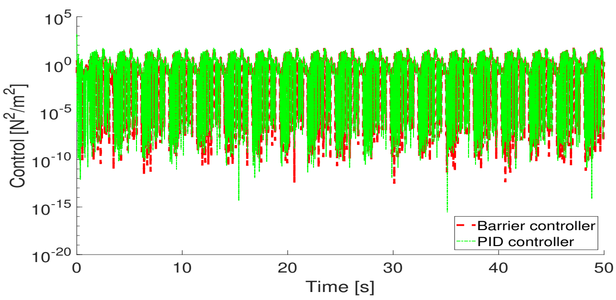

Fig. 5. Logarithmic comparison of the control norm signal between the proposed and the PID controllers for the hip articulation.

Figures 7 and 8 shows the time evolution of the tracking error norm of the reference trajectories. Such simultaneous depicting confirms that the provided controller enforces the tracking of the reference trajectories as well as the PID does, but ensuring the fixed time convergence and the satisfaction of the state restrictions. Notice that such conditions also limits the available control energy which can be used to track the reference trajectories. Despite of this negative condition,

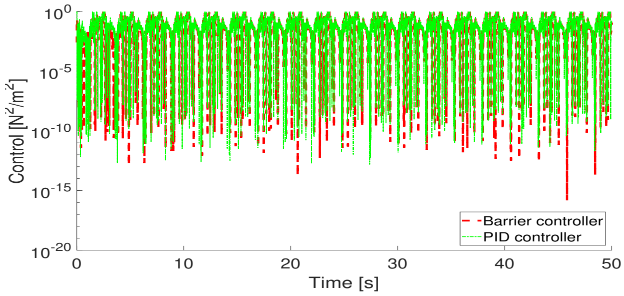

Fig. 6. Logarithmic comparison of the control norm signal between the proposed and the PID controllers for the knee articulation.

the proposed controller succeeds to complete the tracking problem.

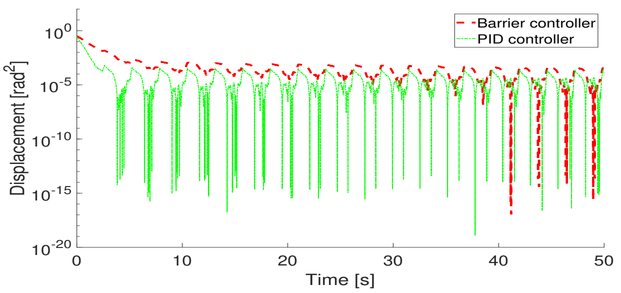

Fig. 7. Logarithmic comparison of the error norm signal between the proposed and the PID controllers for the hip articulation.

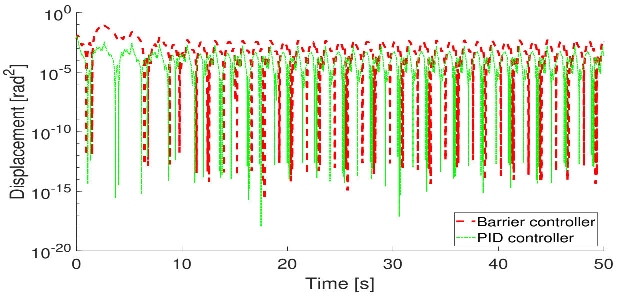

Fig. 8. Logarithmic comparison of the error norm signal between the proposed and the PID controllers for the knee articulation.

In order to evaluate numerically the performance of both controllers, it was obtained the L_2 norm of the control and error signals at each articulation (Table II).

TABLE II
NORM L_2 OF THE ERROR AND CONTROL SIGNALS OF BOTH JOINTS

Characteristics	Controller	
	Barrier	PID
$J_{e,h}$	2.5892×10^4	9.0636×10^3
$J_{c,h}$	7.4752×10^6	9.6471×10^6
$J_{e,k}$	1.8016×10^4	1.1642×10^3
$J_{c,k}$	8.1580×10^5	1.0912×10^6

The evaluation of the performance index J_e was obtained as $J_e = \int_0^{t_f} |e^2(t)|dt$ where e is the vector of errors at the hip and the knee. In the same way, J_c was obtained as $J_c = \int_0^{t_f} |u^2(t)|dt$ where u is the vector of the control signals at the hip and the knee.

The norm $J_{c,h}$ of control signal using the PID controller is 1.2905 greater than the one generated by the proposed control. Alike, the norm of the PID controller for the knee is 1.3376 times bigger than the norm generated by the Barrier controller.

The error signals for the hip and the knee, $J_{e,h}$ and $J_{e,k}$ respectively, generated by the Barrier controller are 2.8567 and 15.4752 times bigger than the generated by the PID controller at each joint.

V. CONCLUSION

This study proposes a new finite time controller for a class of simplified biped robot with state restrictions. The stability analysis yields to obtain the time dependent gain adjusting law which may guarantee the tracking of the reference trajectories. Besides, the application of the proposed controller justified the exerting of a regular gait cycle for a simulated biped robot. The suggested approach is comparable to the tracking results forced by the application of the classical PID controller. However, the suggested controller guarantees the satisfaction of the state constraints.

REFERENCES

[1] M. Vukobratovic and D. Juricic, "Contribution to the synthesis of biped gait," *IEEE Transactions on Biomedical Engineering*, vol. BME-16, no. 1, pp. 1–6, Jan 1969.

[2] A. Polyakov and L. Fridman, "Stability notions and lyapunov functions for sliding mode control systems," *Journal of the Franklin Institute*, vol. 351, no. 4, pp. 1831–1865, 2014.

[3] A. Levant, "On fixed and finite time stability in sliding mode control," in *52nd IEEE Conference on Decision and Control*. IEEE, 2013, pp. 4260–4265.

[4] V. Utkin, *Sliding Modes in Control and Optimization*. Springer-Verlag, 1992.

[5] F. Bejarano and L. Fridman, "High order sliding mode observer for linear systems with unbounded unknown inputs," *International Journal of Control*, vol. 83, no. 9, pp. 1920–1929, 2010.

[6] Y. Shtessel, C. Edwards, L. Fridman, and A. Levant, *Sliding Mode Control and Observation*. Springer New York, 2014.

[7] W.-J. Cao and J.-X. Xu, "Nonlinear integral-type sliding surface for both matched and unmatched uncertain systems," *IEEE Transactions on Automatic Control*, vol. 49, no. 8, pp. 1355–1360, 2004.

[8] B. Bandyopadhyay and D. Fulwani, "High-performance tracking controller for discrete plant using nonlinear sliding surface," *IEEE Transactions on Industrial Electronics*, vol. 56, no. 9, pp. 3628–3637, 2009.

[9] Z. Zuo, "Non-singular fixed-time terminal sliding mode control of nonlinear systems," *IET control theory & applications*, vol. 9, no. 4, pp. 545–552, 2014.

[10] A. Polyakov, D. Efimov, and W. Perruquetti, "Finite-time and fixed-time stabilization: Implicit Lyapunov function approach," *Automatica*, vol. 51, pp. 332 – 340, 2015.

[11] H. Obeid, L. M. Fridman, S. Laghrouche, and M. Harmouche, "Barrier function-based adaptive sliding mode control," *Automatica*, vol. 93, pp. 540–544, 2018.

[12] D. A. Neumann, *Kinesiology of the musculoskeletal system-e-book: foundations for rehabilitation*. Elsevier Health Sciences, 2013.

[13] A. D. Ames, "Human-inspired control of bipedal walking robots," *IEEE Transactions on Automatic Control*, vol. 59, no. 5, pp. 1115–1130, 2014.

[14] N. Martínez-Fonseca, L. Á. Castañeda, A. Uranga, A. Luviano-Juárez, and I. Chairez, "Robust disturbance rejection control of a biped robotic system using high-order extended state observer," *ISA transactions*, vol. 62, pp. 276–286, 2016.

[15] H.-K. CHIANG, J. S. TSAI, and Y.-Y. SUN, "Extended ackermann formula for multivariable control systems," *International Journal of Systems Science*, vol. 21, no. 11, pp. 2113–2127, 1990.

[16] A. Polyakov, "Nonlinear feedback design for fixed-time stabilization of linear control systems," *IEEE Transactions on Automatic Control*, vol. 57, no. 8, pp. 2106–2110, 2011.